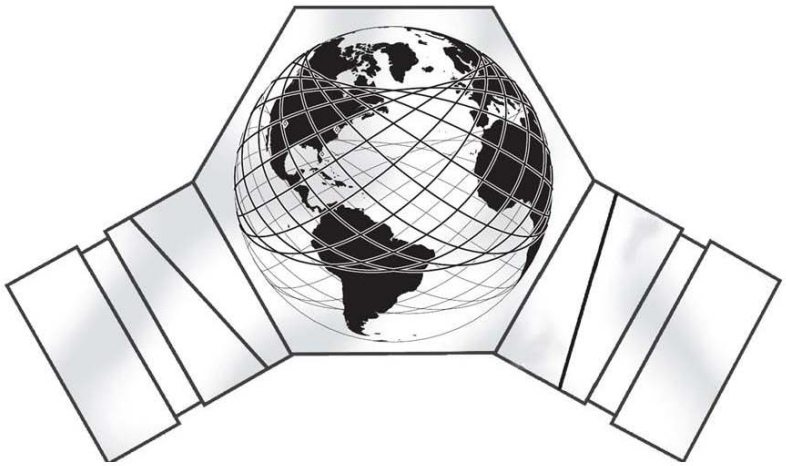

Users Guide to Data from the Spatial Heterodyne Imager for Mesospheric Radicals (SHIMMER)

David E. Siskind
Michael H. Stevens
Christoph R. Englert
Space Science Division, Naval Research Laboratory, Washington DC

November 24, 2014

This work was funded by the NASA Heliophysics Data Environment Enhancements Program

Table of Contents

1. Overview of the SHIMMER mission 3

2. The SHIMMER OH data 3

2.1 Overview 3

2. 2 The “showstat” Summary Plots 5

2.3 Details of the SHIMOH Files 6

3. The SHIMMER PMC Data 6

3.1 Overview 6

3.2 The Map and Summary Figures 7

3.3 Output Data Files 8

4. References 11

Appendix A: OH Summary Plots 12

Appendix B: PMC Maps and Summary Figures 24

1. Overview of the SHIMMER mission

The Spatial Heterodyne Imager for MEsospheric Radicals (SHIMMER) was launched on 7 March 2007, ended its mission in 24 October 2009 [Englert et al., 2008; 2010], and during this time delivered two data products which are archived and described here. First, SHIMMER obtained mesospheric hydroxyl (OH) radiance profiles of solar resonance fluorescence near 309 nm. These were inverted to retrieve OH density profiles between 60 and 90 km. Second, SHIMMER observed Polar Mesospheric Clouds (PMCs) from the enhanced scattering of sunlight from ice particles in the upper mesosphere [Stevens et al., 2009; 2010].

Near each equinox, the STPSat-1 satellite executed a yaw maneuver such that SHIMMER's look direction, which is perpendicular to the satellite velocity vector, was generally oriented toward the summer hemisphere. Considering the relatively low orbital inclination of the satellite (35.4^o), a total range of about 75^o of latitude were observed at any one time. As a result, tropical data are available throughout the mission whereas data from mid-latitudes are only available in the summer hemisphere since the instrument was pointed in that direction. For OH, radiance profiles were averaged dailyand grouped by latitude (northern tropics (0-15^o N) and northern mid-latitudes (50-58^o N)). The data are furthermore grouped by orbit node (ascending and descending), which effectively separates the observations into the local time intervals of each node. For PMCs, the SHIMMER viewing geometry led to extensive annual coverage equatorward of 58^o latitude in both hemispheres, representing the equatorward edge of this primarily polar phenomenon.

This manual describes both data products including the range of coverage and their limitations. Section 2 describes the OH data and Section 3 describes the PMC data.

2. The SHIMMER OH data

2.1 Overview

OH data were obtained by imaging the limb every 20 s between 58°N and 58°S. These radiance profiles were inverted to retrieve daily averaged mesospheric OH densities between 60 and 90 km in 2 km increments. A total of 1816 OH profiles are available, 881 from the ascending (A) portion of the orbit and 935 from the descending (D) portion of the orbit. Because the satellite is moving eastward at latitudes between 50°N and 58°N, the profiles from the A portion are about 3 hours earlier in local solar time than the D portion in this latitude band. The OH number density profile data are stored in directories for the tropics ("0_to_15N") and for the mid-latitudes ("50N_to_58N"). Below we give an overview of the available data. Section 2.2 describes the plots which summarize the viewing conditions for each period of data taking and Section 2.3 below describes the specific format of the OH data files.

The SHIMMER OH observations are grouped into 6 periods of data taking for the ascending and descending nodes in each of the three years of the SHIMMER mission. The number of inverted profiles for each period and each portion of the orbit (A or D) is given below.

2007: tropics: 165 (A) and 166 (D), from days 99-365 (9 April through 31 December)
2007: mid-latitudes: 114 (A) and 134 (D), from days 95-268 (5 April through 25 September)
2008: tropics: 202 (A) and 211 (D), from days 1-363 (1 January through 28 December)
2008: mid-latitudes: 111 (A) and 123 (D), from days 119-339 (28 April through 4 December)
2009: tropics: 189 (A) and 187 (D), from days 13-267 (13 January through 24 September)
2009: mid-latitudes: 100 (A) and 114 (D), from days 111-267 (21 April through 24 September)

The mid-latitude periods always have less data than the tropical periods due to the yaw cycle of the spacecraft indicated above. An analysis of the mid-latitude data was given by Siskind et al. [2013]. The tropical data have not been quantitatively studied heretofore.

Data taking started around day 95 in 2007 and stopped on day 267 in 2009. There are missing days, which are preferentially distributed around the equinox yaw periods during which the spacecraft lost pointing information. A list of day numbers for each year with missing data within the above periods follows:

2007 Tropics:
A: 99, 102, 105, 129-132,134, 146-154, 173, 176-178, 197-202, 212, 217, 221-227, 232,247-251, 282, 285-334,338-343,364-365, 100 total missing days

D: 126-127, 129-132,134,142,146-153, 173, 176-178,196-202,217,221-224,227,232,247-252,263,282,285-334,338-343 98 total missing days

2007 Mid-Lats:
A: 97-98, 105, 111-134, 164-175, 215-228, 232, 263-268
60 total missing days
D: 97-98, 105, 118-134, 171-174, 167-177, 179-180, 217, 220-227, 231-232, 263
51 total missing days

2008 Tropics:
A: 1-18, 35, 49-69, 90-118, 129, 138-141, 189-192, 240-244, 246-248, 260-273, 275, 281-283286, 288-325, 327-328, 333-335, 337-339, 354-363, 161 total missing days
D: 7-17, 35, 49, 57-68, 90-118, 120, 129, 135-142, 186-193, 234, 238-244, 247-248, 261-273, 275, 281-283, 286, 288-325, 327-329, 333-349, 354-357, 152 total missing days

2008 Mid-Lats:
A: 119, 129, 139, 158-168, 208-221, 243-244, 247-248, 256-275, 281-336, 338-339
110 total missing days
D: 124, 139, 163-168, 172-173, 213-219, 225-226, 243-244, 247-248, 260-275, 281-338
96 total missing days

2009 Tropics:
A: 22, 38-60, 89-90, 92-99, 102-103, 129-133, 160, 180-183, 197-202, 210-218, 231-235,
66 total missing days

D: 22, 38-43, 49-60, 64, 67, 89-90, 100-103, 127-134, 161, 177-184, 197-202, 210-219, 229-236 66 total missing days

Mid-Lats:

A: 111, 148-160, 196-218, 247-266 57 total missing days

D: 115, 154-158, 163-164, 196-202, 205-218, 253-266 43 total missing days

2. 2 The "showstat" Summary Plots

These are plots summarizing relevant viewing conditions for each of the 6 data periods documented above. Thus, there are a total of 12 figures representing each data period (ascending and descending nodes). They are included as Appendix A and labeled according to "yyyy_start_lat_end_lat_node" where startlat is either 00 or 50 and endlat is either 15 or 58 and node is either A(ascending) or D(descending)

Each of the figures has 6 panels. Starting down the columns from the upper left for each figure:

a) Number of spectra obtained on each day. Typically hundreds of OH radiance spectra are obtained, fitted, and averaged together daily prior to inversion to produce a single density profile.
b) Solar zenith angle (SZA) (middle left). OH densities are sensitive to the solar zenith angle and the daily average as well as the range of zenith angles are shown.
   Note that the number of spectra goes to zero as the solar zenith angle approaches 90 degrees. This reflects the fact that OH is only observed during day time and thus spectra can only be obtained for SZA < 90.
c) (lower left side panel) Solar scattering angle (SSA). This is defined as the supplement of the angle between the vector from the sun to the limb tangent point and the limb tangent point to the satellite. Thus, a SSA greater than 90° represents a backward scattering geometry, where the sun is behind SHIMMER as it looks toward the tangent point. Conversely, a SSA less than 90° is a forward scattering geometry.
d) (Upper right side panel) Latitude of the limb tangent point (upper right). Since these periods were pre-selected for a narrow latitude range, the scatter of the points will be in that narrow range.
e) Local solar time (LST) at the tangent point. Because SHIMMER measures OH solar resonance fluorescence, observations are only made during the day. Note that the sampling precesses to earlier local times at about 30 minutes per day. For the mid-latitude scans, the daylit hours are sampled roughly 3 times per season. When the SZA is greater than 90^o, the LST is typically greater than 20 or less than 4 at mid-latitudes and there is often a gap in the data (due to lack of sunlight). The number of spectra (upper left panel) will then be zero.
f) (lower right side panel) Altitude range of the limb observation. Nominal altitudes are from 35-100 km for each limb image. This is governed by the field of view of the instrument projected onto the limb. On occasion, SHIMMER was pitched up to search for a OH signal at higher altitudes. Thus there are scans which go from either about 45-110 km (common in 2008) or 65-130km (for example, in early June 2007 or late in 2009). When no

observations were made there is no range of altitudes indicated. This panel is also useful for getting a quick overview of when OH data might have been taken.

2.3 Details of the SHIMOH Files

The OH density profiles are contained in files which are labeled "shimoh_yyyy_ddd_node.out" where, "yyyy" is the year, "ddd" is the day of year and "node" is either A or D for ascending or descending node. Thus, there are often two files per day, each representing the averaging of many dozens of radiance profiles. Each shimoh file contains a 4 point header:
NDIM LST SZA LAT

Where NDIM is the number of points in the altitude profile, LST is the local solar time of the measurement, SZA is the solar zenith angle, and LAT is the mean latitude, respectively. As noted above in Section 1, since the descending node of the orbit is to the east of the ascending node, for a given day, the LST for the "_D.out" files will typically be 1-4 hours later than for the "_A.out" files.

The data follow in 5 columns: altitude, OH densities, uncertainty in the OH densities (1σ), OH radiances (uninverted intensities along the line of sight), and uncertainty in the OH radiances. The number of altitudes (keyed to the value of NDIM above) will vary depending upon the goodness of the fit to the OH spectra, but often goes from 60-82 km in 2 km intervals. Due to the typically sharp decrease of OH abundance above 80 km and the resultant loss of signal, the highest altitude will typically have a radiance error (column 5) exceeding the actual radiance. Since the range of altitudes that the file contains data for reflects the altitudes where the OH number densities can be retrieved, this range will be less than that indicated in Section 2f. See Englert et al. [2010] for further details.

3. The SHIMMER PMC Data

3.1 Overview

Details of the retrieval of PMC can be found in Stevens et al., [2009]. The SHIMMER PMC data are derived from over a million limb images during its three year mission. However, as mentioned earlier, during the periods near the equinoctial yaw maneuvers, pointing information was often limited. This was particularly true for the yaw in Northern autumn, so data from September through November for each year are not included herein. This does not significantly affect PMC statistics since they are primarily a summertime phenomenon. All the remaining images were checked for and, if possible, corrected for measurement artifacts, e.g. detector signals from energetic particles or pointing anomalies; however, with such a large database, a very small,

residual number of corrupted images might still be present. Since reports of PMC equatorward of 30° latitude are almost non-existent in the historical record and also extremely sparse in the SHIMMER data, we have removed all of these observations from the PMC database in order to minimize the number of spurious detections.

The remainder of the PMC observations were assessed for anomalies with particular attention given to observations equatorward of 45° latitude, which is a region that is typically inhospitable to PMC formation. If the shape of a PMC altitude profile was inconsistent with a typical PMC profile it was removed from the database. The same tests were applied to all observations at all latitudes. Published SHIMMER PMC results are not significantly affected by this final assessment of the database [Stevens et al., 2009; Eckermann et al., 2009; Stevens et al., 2010; Siskind et al., 2011; Russell et al., 2014]. Section 3.2 below describes the summary figures as well as annual PMC occurrence maps and Section 3.3 describes the individual PMC data files.

3.2 The Map and Summary Figures

The data are divided into three different directories representing each year of operations: 2007, 2008 and 2009. In each of these directories there are two figures summarizing the SHIMMER PMC observations. Both these figures are included here as Appendix B.

The first figure for each year is map_YYYY.ps, where YYYY represents the year. This shows the geographic location of each detected PMC, without regard to when it was detected. Note how the detections for each year are clustered to the highest latitudes observed by SHIMMER (50°-58°). Also indicated on the maps are the total number of images tested for a PMC as well as the total number of PMC detected for each year (775 for 2007, 1211 for 2008 and 1014 for 2009). Although the latitudes sampled in the north and south are the same, there are fewer PMC detected in the south due to higher temperatures there [e.g. Hervig et al., 2013].

We define the occurrence of PMC in the SHIMMER dataset in two ways: one with a higher detection threshold and one with a lower threshold. The lower threshold is used for the detection of all PMC by SHIMMER whereas the higher threshold is used for interpretation of PMC variability over the diurnal cycle. In the latter case, the solar scattering angle varies with local time and the detection threshold is adjusted upward at lower solar scattering angle so that SHIMMER is equally sensitive to PMCs at each point of the diurnal cycle [see Stevens et al. [2009] for further details]. The number of detections using this threshold are labeled as “PMC Thr” on the maps. The points on the map represent the total number of PMC observed using the lower threshold.

We also indicate the number of PMC detected by SHIMMER between 30°-45° latitude for each year on the maps. We find 2 in 2007 (0.3% of all PMC for that year), 5 in 2008 (0.4%) and 4 in 2009 (0.4%). We note that one of these low latitude detections in 2007 was reported by Eckermann et al. [2009].

The second figure (summary_YYYY.ps) shows a time series of some important results of the analysis. The figure contains four panels. In the upper left the number of SHIMMER images tested for PMC each day is indicated. As discussed above, images are removed if they are at low latitudes (<30°) or if there is uncertainty in the pointing for a given image. Since SHIMMER can only measure during the day, the oscillation of the daily images used is primarily a function of the changing lighting conditions at the tangent point.

In the bottom left we show a time series of PMC detections for the year in question. Note that they are strongly clustered in the summertime. In the upper right we show a time series of thresholded PMC detections, which can be used when assembling the observations in local time as discussed above. The observed PMC peak in the middle of the year is primarily due to the lower temperatures near solstice and their variation during this time is primarily due to the slowly varying local time at the tangent altitude over the PMC season [Stevens et al., 2009].

In the bottom right we show a time series of PMC altitudes, defined as the altitude of peak brightness. We note that there are inherent limitations to identifying the peak brightness of a PMC when in a limb viewing geometry. As a result, this peak will have a low bias since occasionally the signal could originate from the foreground or background rather than the tangent altitude. For those PMC reported between 78-80 km we regard this bias to be evident since PMC are historically almost never reported at those altitudes.

3.3 Output Data Files

SHIMMER PMC data ASCII files are provided for each day of the observations. The naming convention for the files is “all_file_YYYY_DOY.out” where “YYYY” indicates the year (2007, 2008 or 2009) and “DOY” indicates the day of year (001 to 366). All SHIMMER altitudes are adjusted upward for a pointing offset of 2.81±0.35 km as discussed in Englert et al. [2008].

Each of these files has a five line header. The first line indicates the year and day of year of the data. The second line indicates the total number of PMC detected on that day. The third line (“PMCs Detected above Higher Threshold”) indicates the number of PMC detected when using a phase function of the ice particles as discussed above. Since SHIMMER also detects OH [Englert et al., 2010] we include OH radiances at two altitudes observed simultaneously with each image and this is stated in the fourth line (“OH Radiances at 80 and 87 km”). The OH radiances are included because, even though the full inversion often does not extend above 80 km, at these altitudes the radiance is directly proportional to the OH density [cf. Englert et al., 2010; Figure 14]. In turn, the OH density is a proxy for water vapor in the upper mesosphere. Previous observations of OH in the presence of PMC are have indicated enhancements, presumably due to the sublimation of ice particles [Summers et al., 2001]. The chosen altitudes of 80 km and 87 km

bracket the PMC region and are a diagnostic of the local OH number densities there. Throughout the data files, a value of “-99.9” indicates that there is no data relevant to that entry.

The last line of the header labels the 19 columns of output used to describe each SHIMMER image and they are as follows:

YEAR: The year of the observation.

DOY: The day of year of the observation.

GMT: The Greenwich Mean Time given in HH:MM:SS where HH are hours, MM are minutes and SS are seconds.

LAT: The latitude of the tangent point expressed in degrees north from the equator.

LON: The longitude of the tangent point in degrees east.

LST: The local solar time in hours from midnight.

SSA: The solar scattering angle in degrees. This varies between 0 and 180°, where 0° is forward scattering and 180° is backscattering.

SZA: The solar zenith angle in degrees, where 0° is overhead sun.

PMCRAW: Indicates whether a PMC is detected or not. It is either 1 for a detection or 0 for a non-detection.

PMCMIE: Indicates whether a PMC is detected above the applied threshold using a presumed phase function with a dependence on the solar scattering angle as discussed above and in Stevens et al. [2009].

BGRND: This is -99.9 when there is no PMC present. When there is a PMC, this is the average Rayleigh scattered background signal across the SHIMMER passband that is fit to the profile away from the PMC observation (in kR/nm).

BRT: This is -99.9 if no PMC. When there is a PMC this is the background corrected peak brightness of the PMC (in kR/nm).

THRRAW: This is -99.9 if no PMC. When there is a PMC this is the threshold used to identify a PMC. Comparison of BRT to THRRAW indicates how bright the PMC above the threshold.

THRPHS: This is -99.9 if there is no PMC present above the higher threshold used which uses the SSA dependence of PMC ice particle scattering as discussed above. If there is a PMC present above this threshold then this represents the threshold used to detect that PMC (in kR/nm).

PK: This is the altitude of the peak emission (in km).

OH80 (kR): The OH(0,0) solar resonance fluorescence radiance detected by SHIMMER at 80 km tangent altitude (in kR).

OHE80: The uncertainty (1σ) for the 80 km OH radiance (in kR).

OH87 (kR): The OH(0,0) solar resonance fluorescence radiance detected by SHIMMER at 87 km tangent altitude (in kR).

OHE87: The uncertainty (1σ) for the 87 km OH radiance (in kR).

4. References

Eckermann, S.D., , K.W. Hoppel, L. Coy, J.P. McCormack, D.E. Siskind, K. Nielsen, A. Kochenash, M.H. Stevens, C.R. Englert, M. Hervig, High-Altitude Data Assimilation System Experiments for the Northern Summer Mesosphere Season of 2007, J. Atm. Sol.-Terr. Phys., 71, 531-535, 2009.

Englert, C.R., M.H. Stevens, D.E. Siskind, J.M. Harlander, F.L. Roesler, H.M. Pickett, C. von Savigny and A. Kochenash, First results from the Spatial Heterodyne IMager for MEsospheric Radicals (SHIMMER): The diurnal variation of mesospheric hydroxyl, Geophys. Res. Lett., 35, L19813, doi:10.1029/2008GL035420, 2008.

Englert, C.R., M.H. Stevens, D.E. Siskind, J.M. Harlander, and F.L. Roesler, Spatial Heterodyne Imager for Mesospheric Radicals on STPSat-1, J. Geophys. Res., 115, D20306, doi:10.1029/2010JD014398, 2010.

Hervig, M.E., D.E. Siskind, M.H. Stevens and Lance E. Deaver, Inter-hemispheric comparison of PMCs and their environment from SOFIE observations, *J. Atm. Sol.-Terr. Phys.*, 104, 285-298, 2013.

Russell, J.M. III, P. Rong, M.E. Hervig, D.E. Siskind, M.H. Stevens, S.M. Bailey and J. Gumbel, Analysis of mid-latitude Noctilucent Cloud occurrences using satellite data and modeling, *J. Geophys. Res*, 119, doi: 10.1002/2013JF021017, 2014.

Siskind, D. E., M. H. Stevens, M. Hervig, F. Sassi, K. Hoppel, C. R. Englert, and A. J. Kochenash, Consequences of recent Southern Hemisphere winter variability on polar mesospheric clouds, J. Atm. Solar-Terr. Physcs, 73, 2013-2021, 2011.

Siskind, D. E., M. H. Stevens, C. R. Englert, and M. G. Mlynczak, Comparison of a photochemical model with observations of mesospheric hydroxyl and ozone, J. Geophys. Res., 118, 195-207, doi: 10.1029/2012JD017971, 2013.

Stevens, M.H., M. Hervig, S.V. Petelina, W. Singer and K. Nielsen, The diurnal variation of noctilucent cloud frequency near 55° N observed by SHIMMER, J. Atm. Sol.-Terr. Phys., 71, 401-407, 2009.

Stevens, M.H. et al., Tidally induced variations of PMC altitudes and ice water content using a data assimilation system, J. Geophys. Res., 115, D18209, doi:10.1029/2009JD13225, 2010.

Summers, M. E., R. R. Conway, C. R. Englert, D. E. Siskind, M. H. Stevens, J. M. Russell III, L. L. Gordley, and M. J. McHugh, Discovery of a water vapor layer in the Arctic summer mesosphere: Implications for Polar Mesospheric Clouds, Geophys. Res. Lett., 28, 3601-3604, 2001.

Appendix A: OH Summary Plots

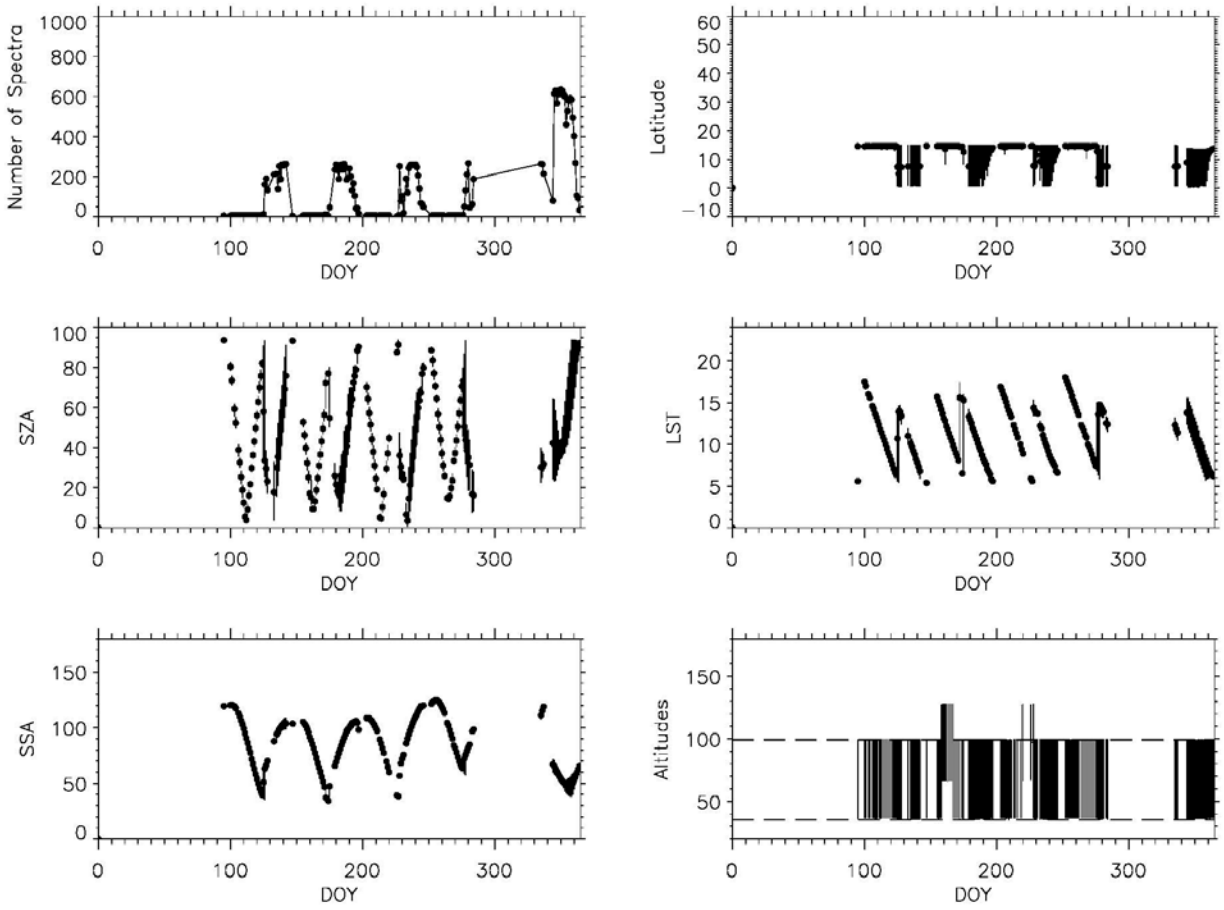

A1: 2007_00_15_A

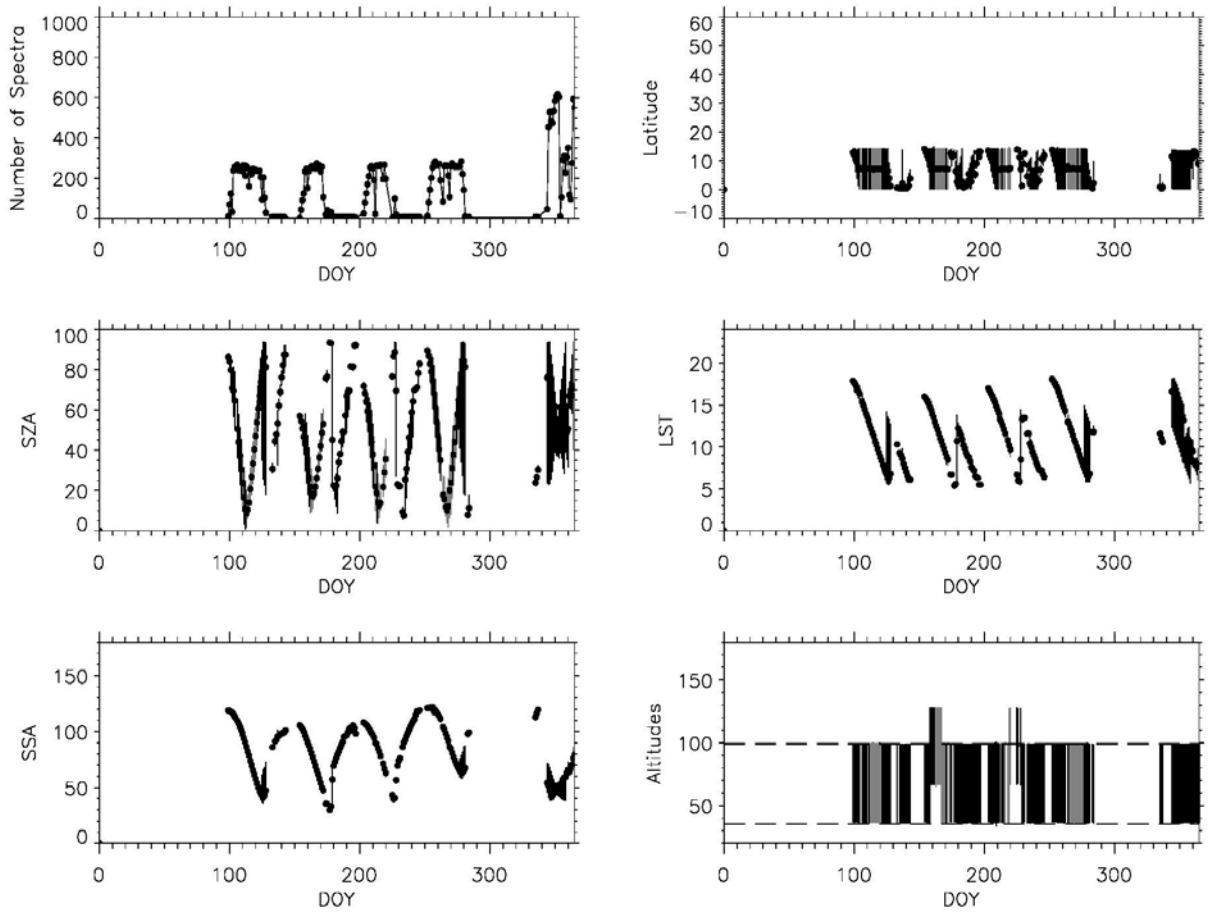

A2: 2007_00_15_D

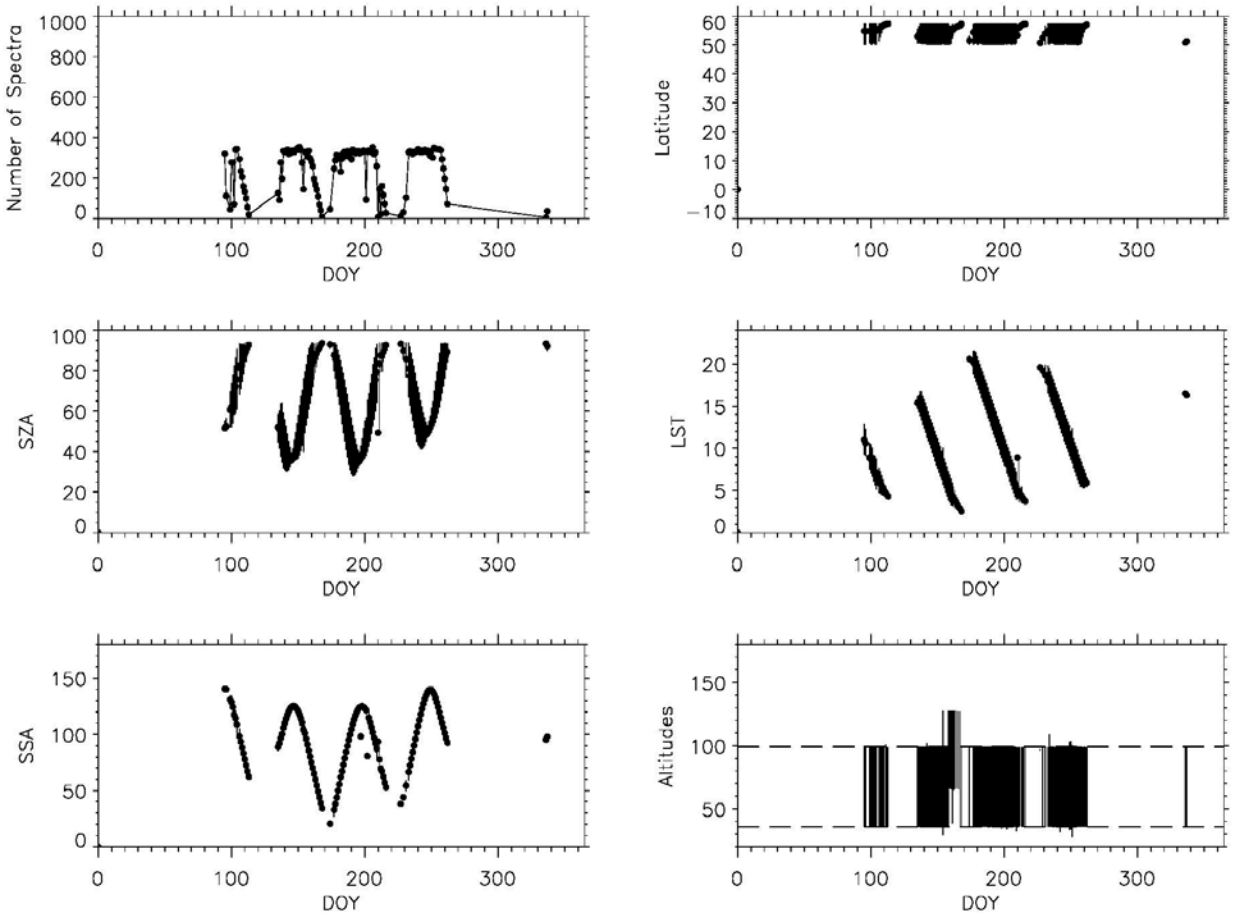

A3: 2007_50_58_A

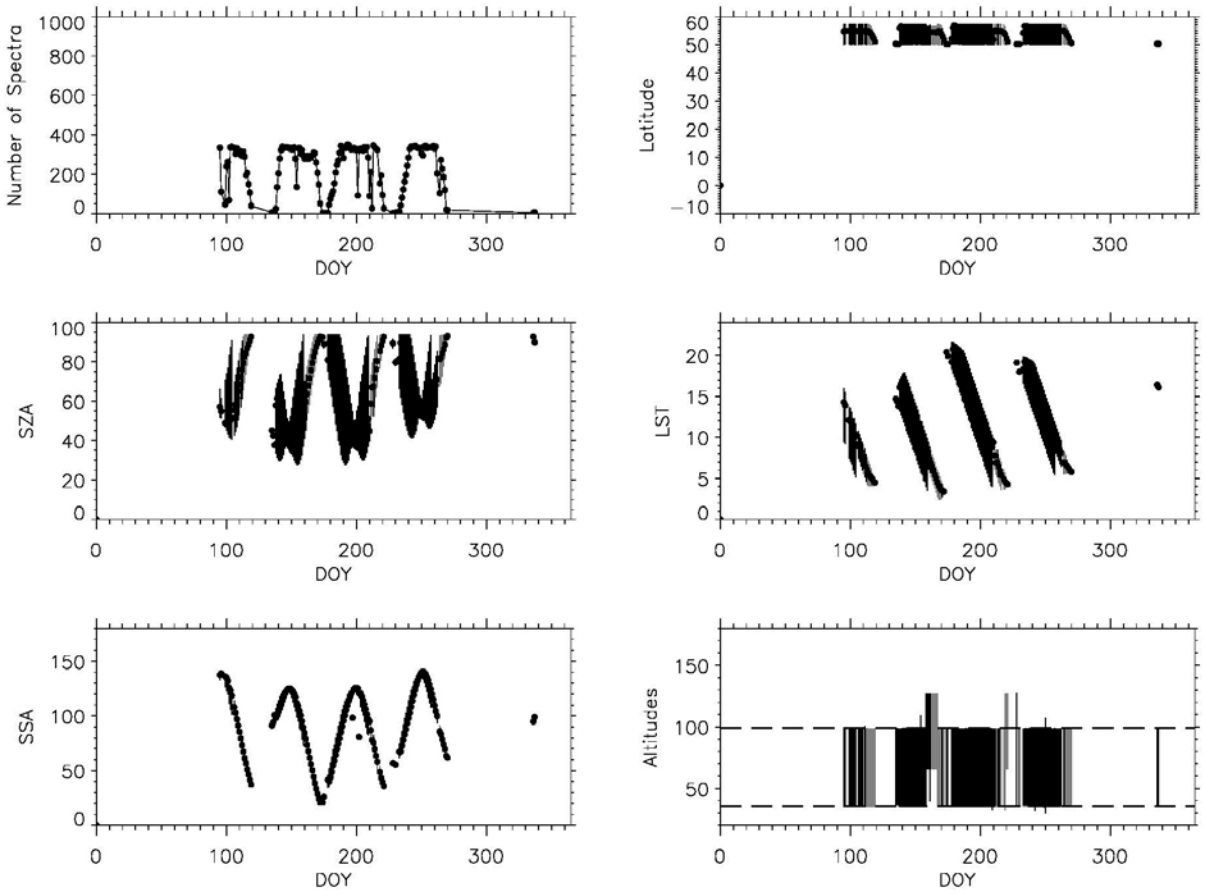

A4: 2007_50_58_D

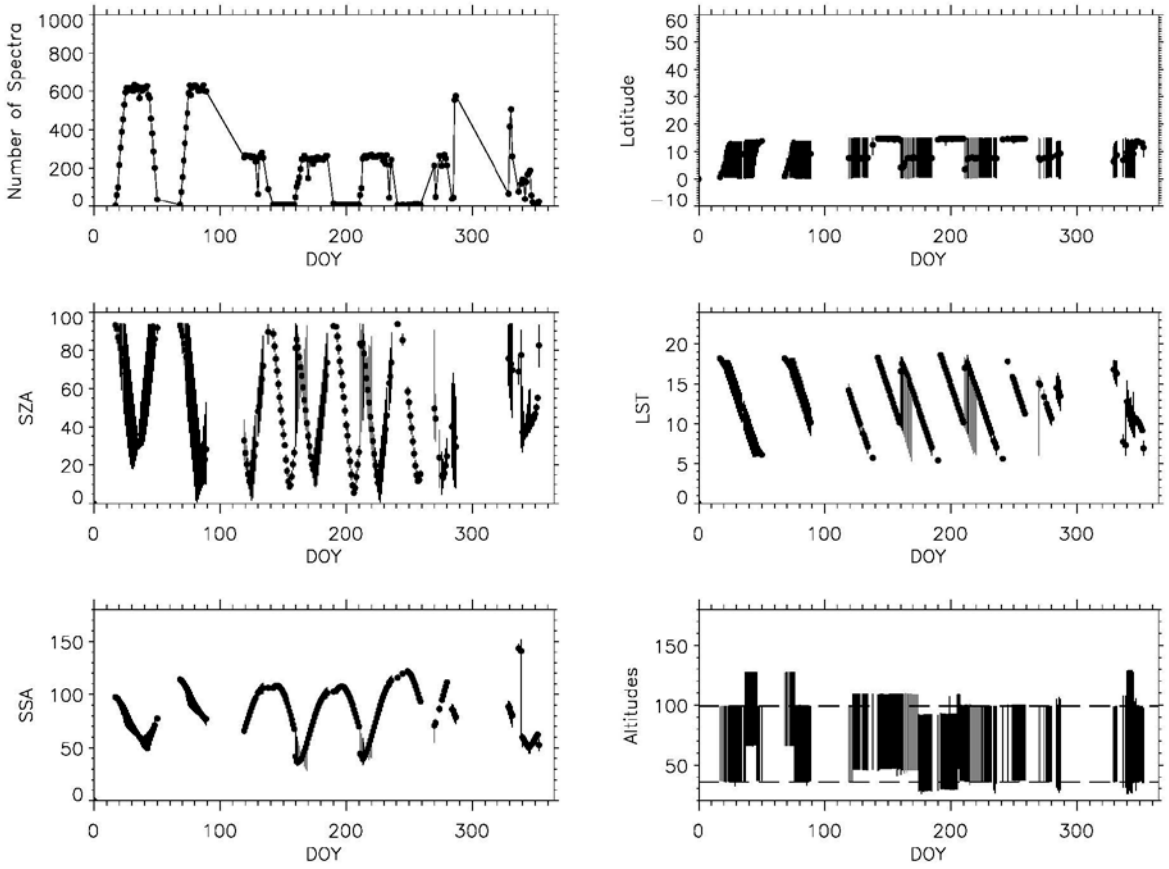

A5: 2008_00_15_A

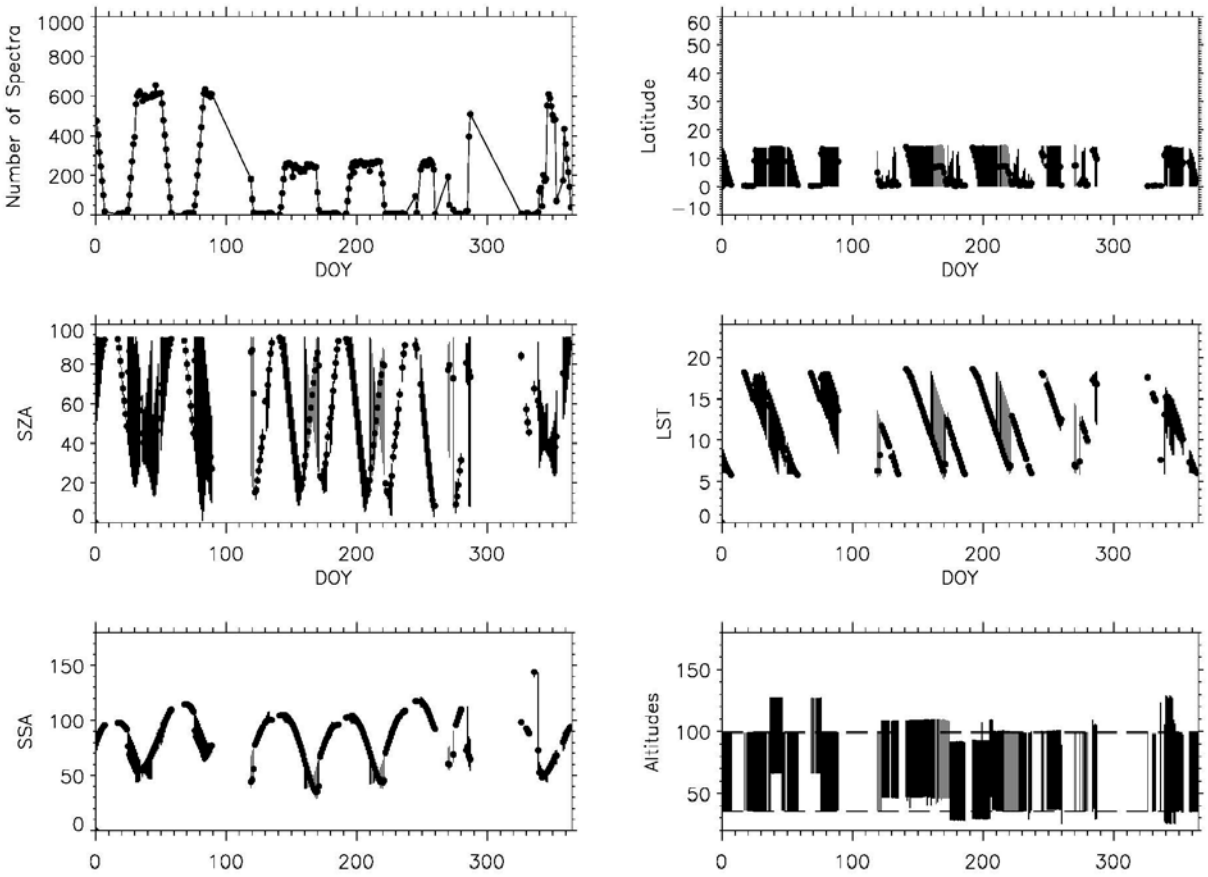

A6: 2008_00_15_D

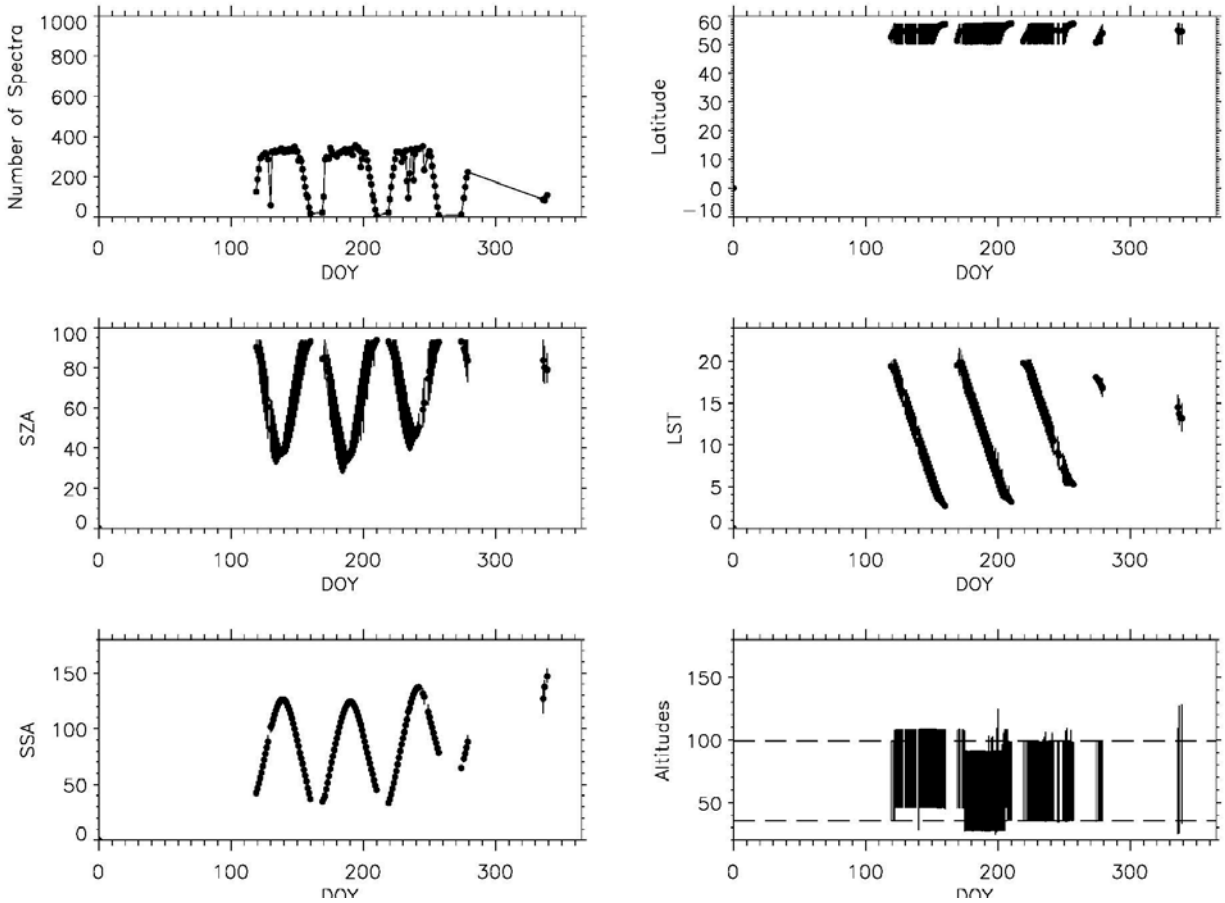

A7: 2008_50_58_A

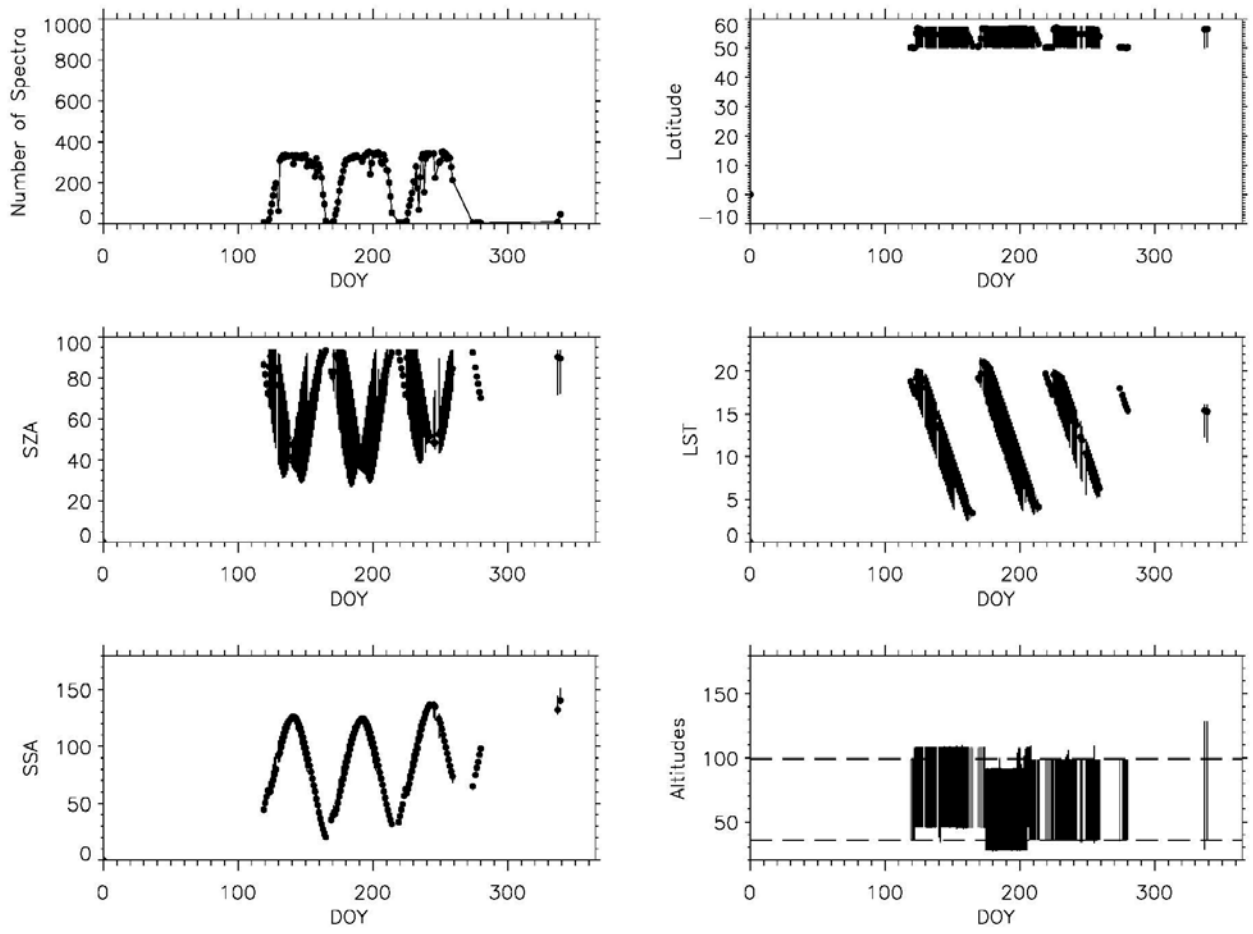

A8: 2008_50_58_D

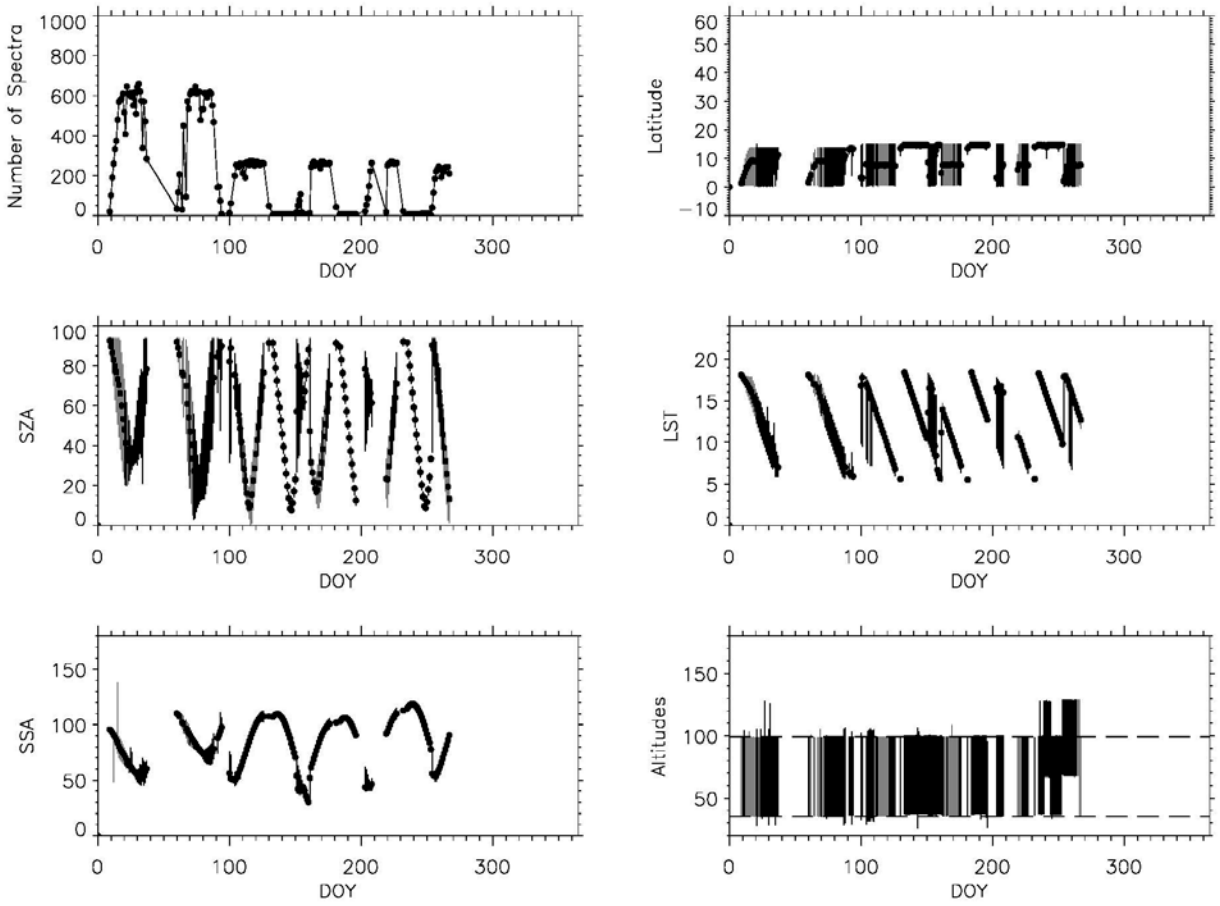

A9: 2009_00_15_A

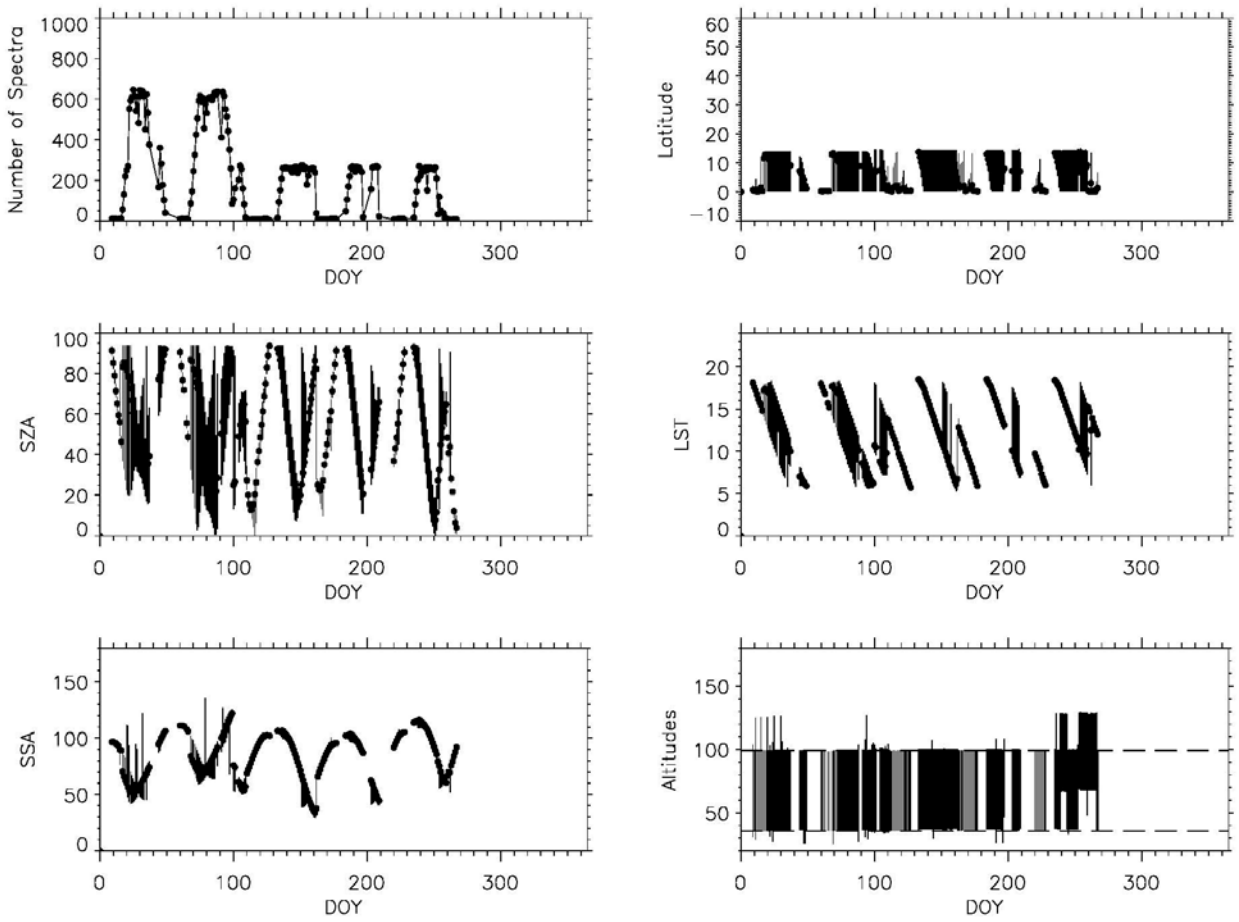

A10: 2009_00_15_D

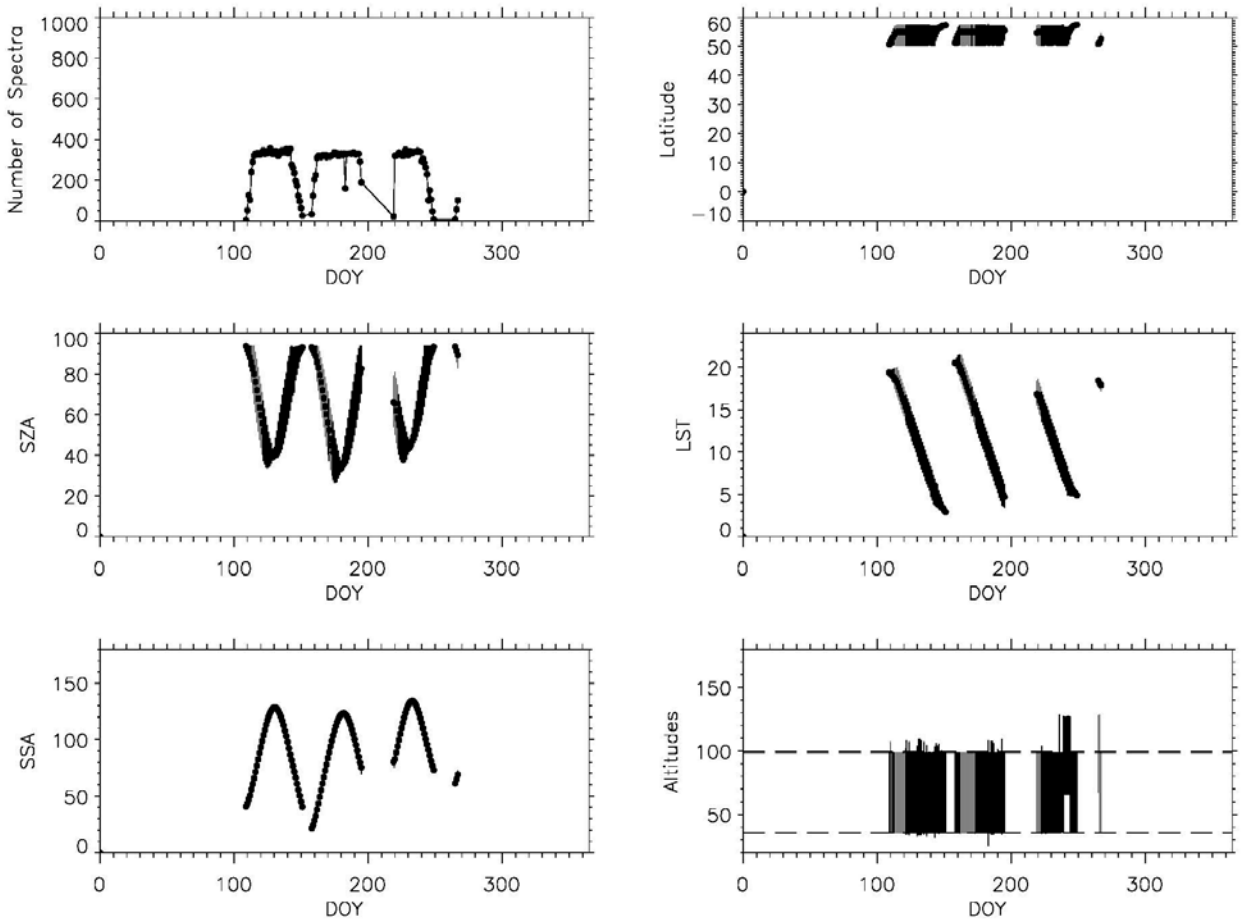

A11: 2009_50_58_A

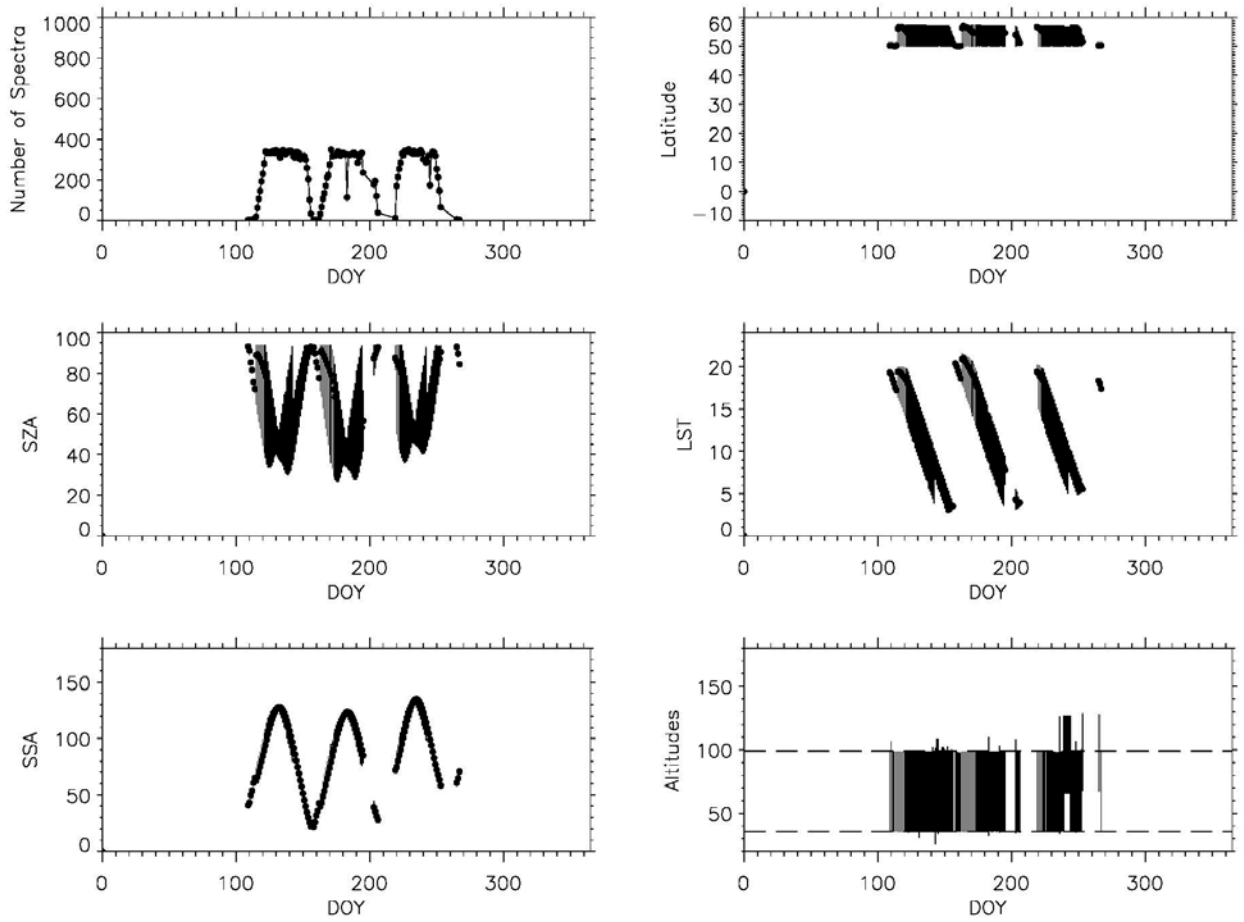

A12: 2009_50_58_D

Appendix B: PMC Maps and Summary Figures

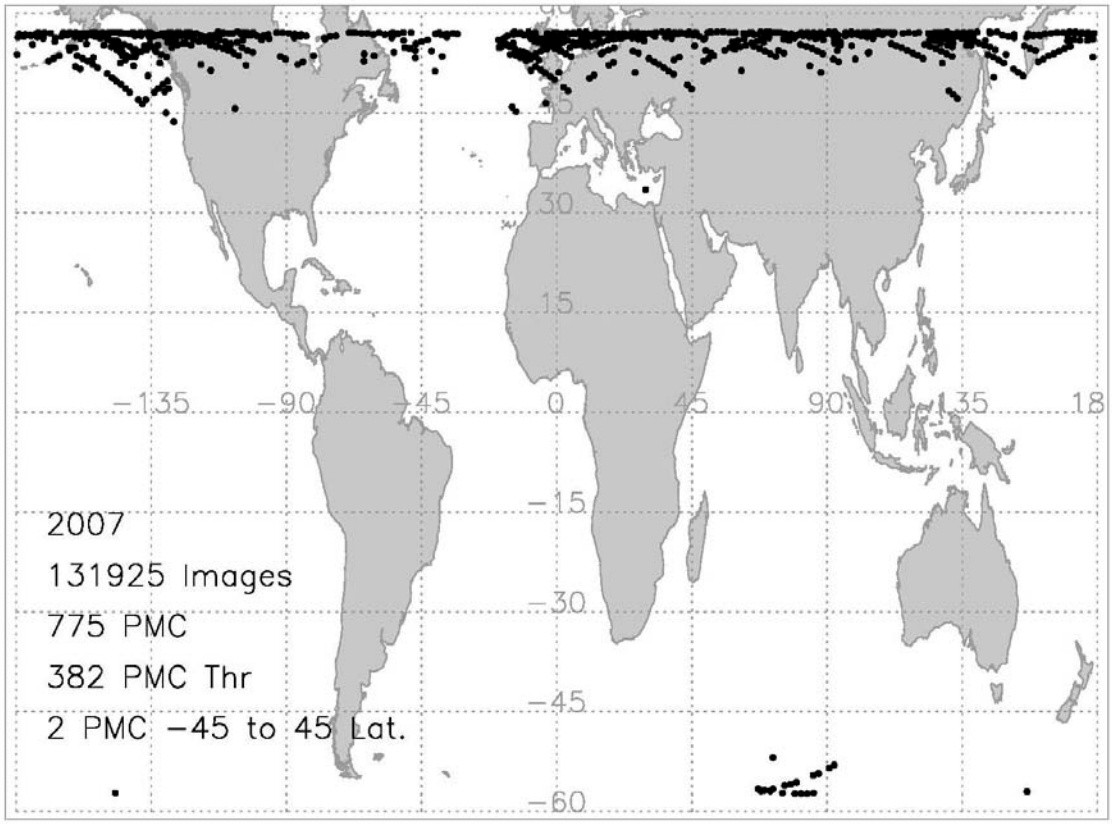

B1: map_2007

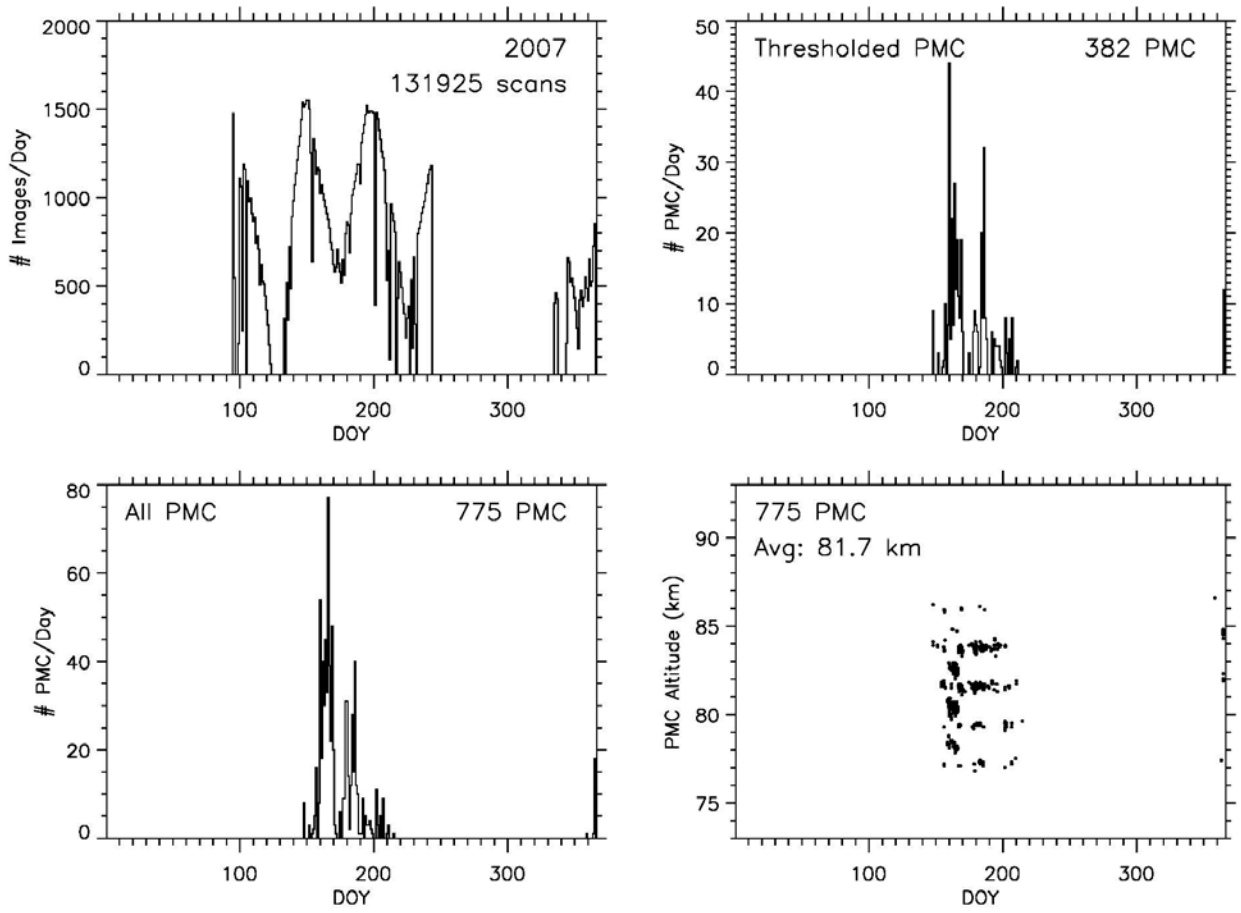

B2: Summary_2007

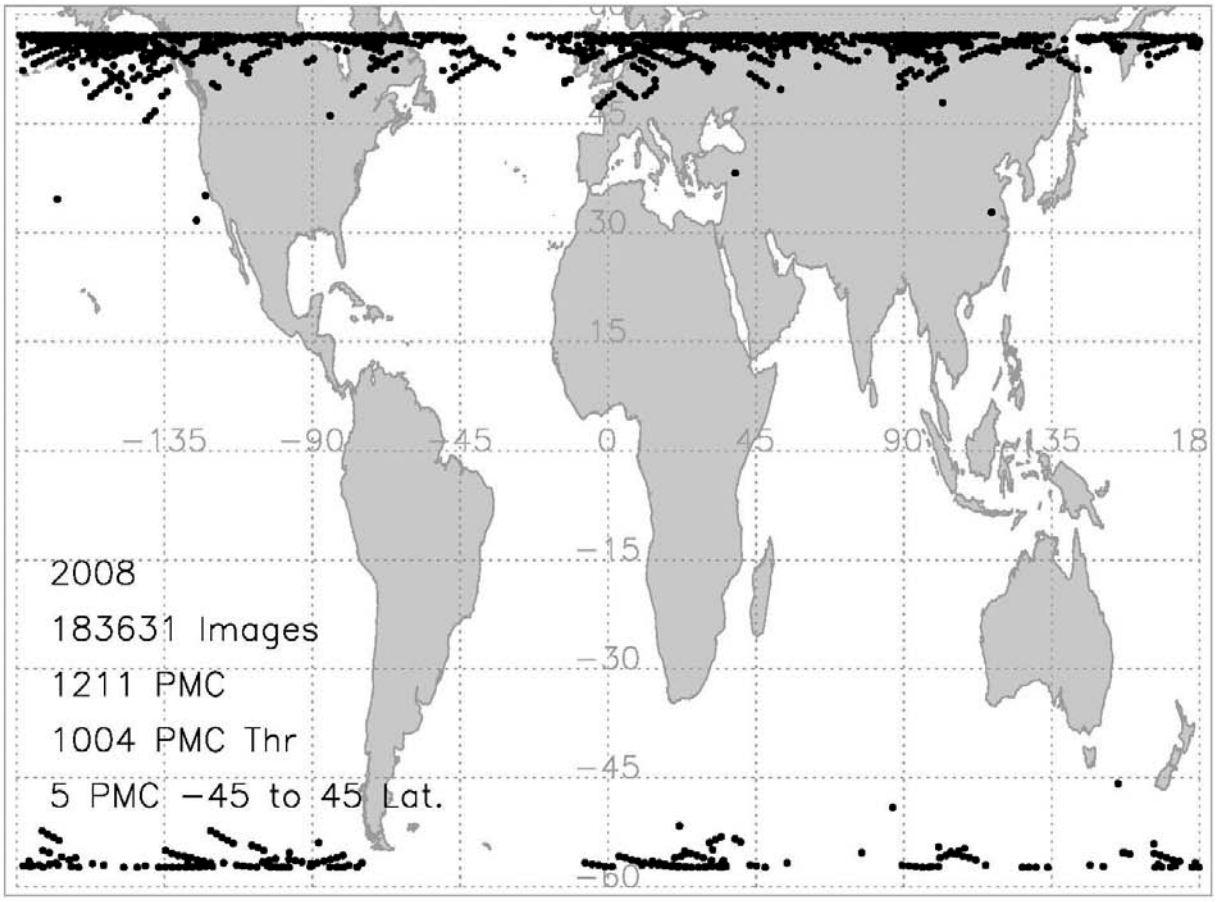
30
15
−135
−90
−45
0
45
90
135
18
−15
−30
−45
−60
2008
183631 Images
1211 PMC
1004 PMC Thr
5 PMC −45 to 45 Lat.

B3: Map_2008

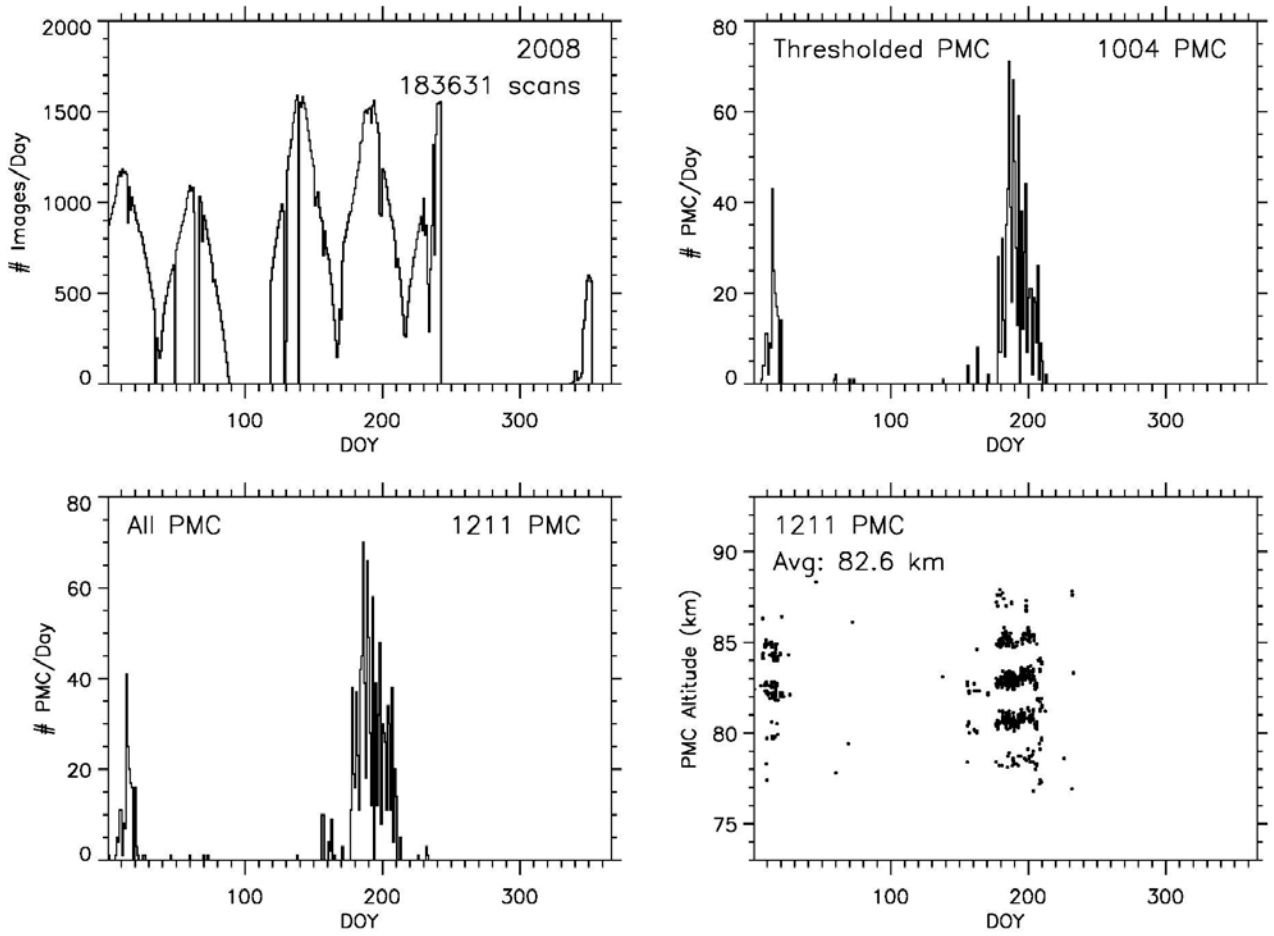

B4: Summary_2008

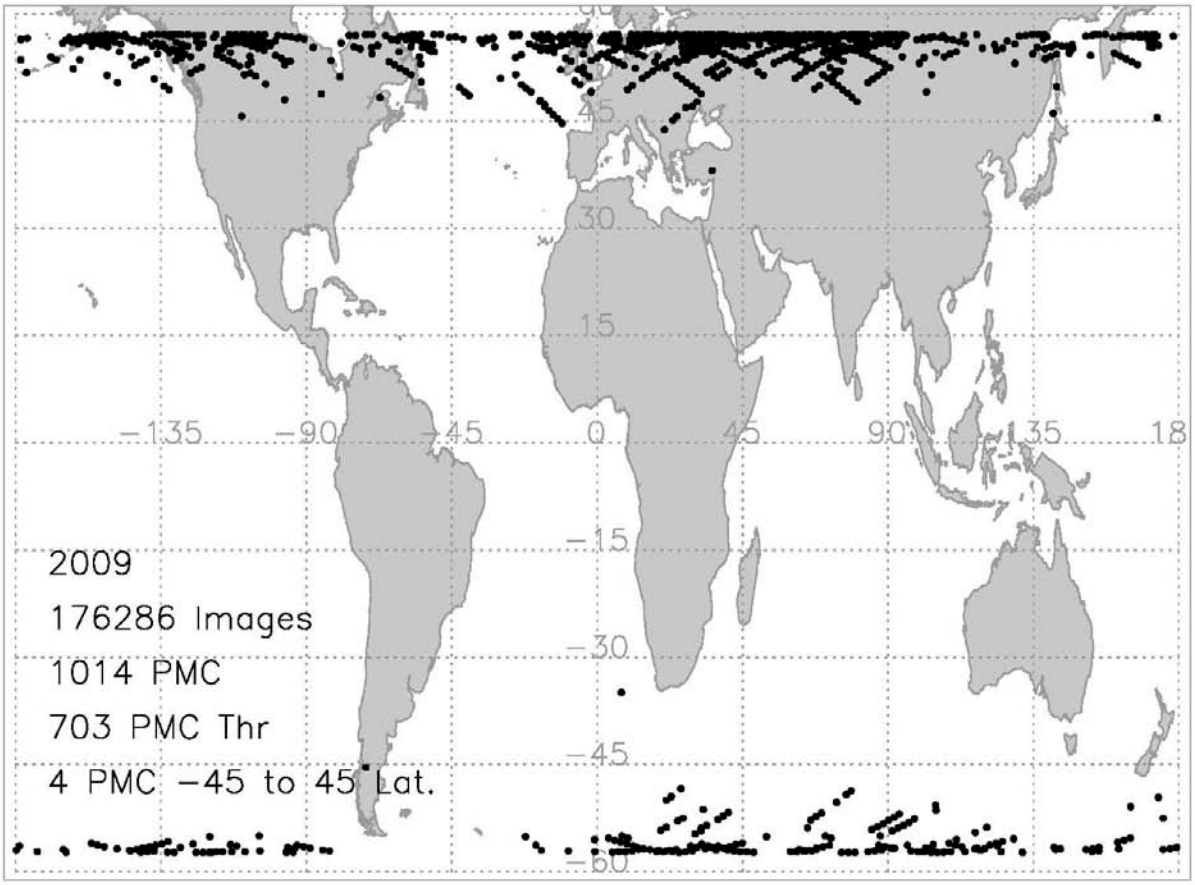
45
30
15
−135
−90
−45
0
45
90
135
180
−15
−30
−45
−60
2009
176286 Images
1014 PMC
703 PMC Thr
4 PMC −45 to 45 Lat.

B5: Map_2009

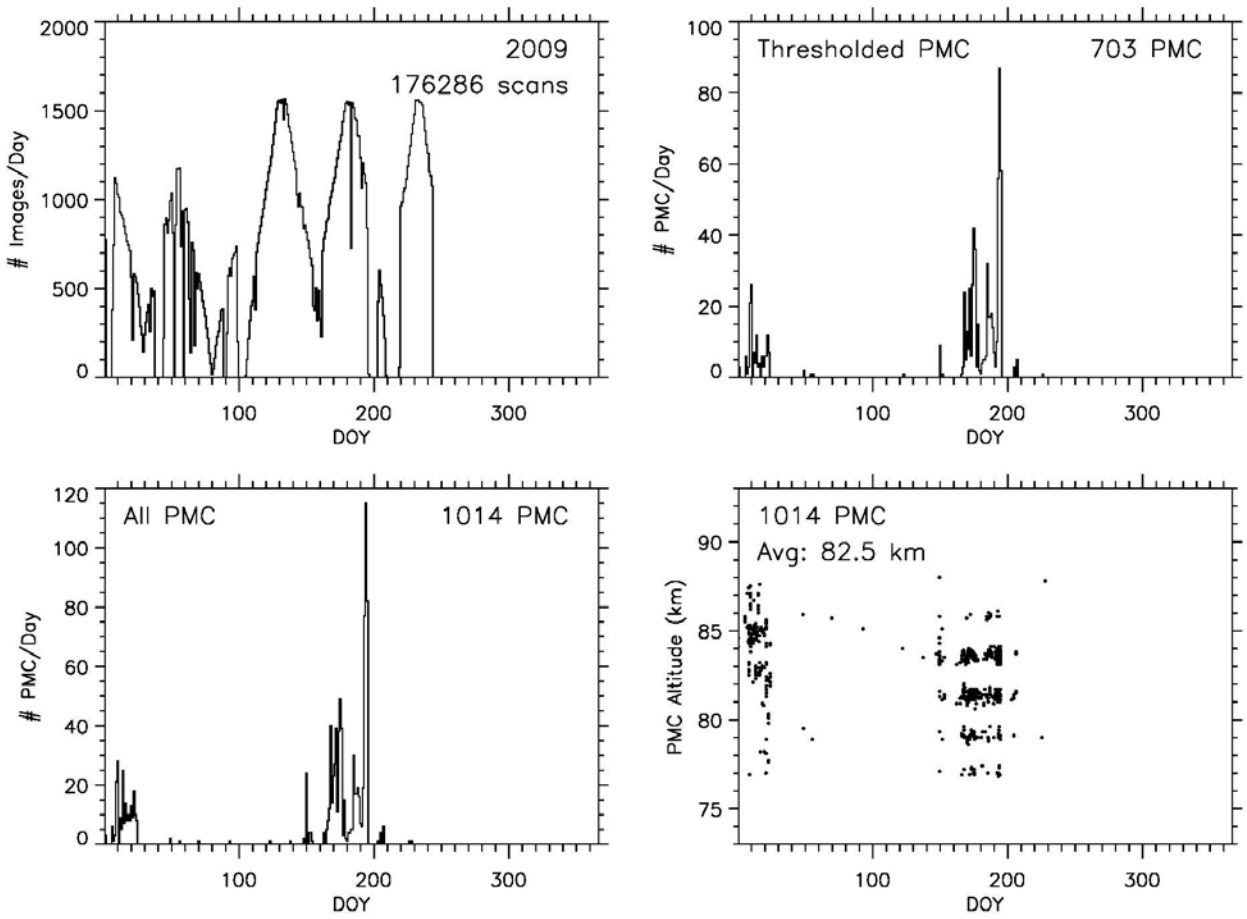

B6: Summary_2009